Food Hydrocolloids for Health 2 (2022) 100049

Contents lists available at ScienceDirect

Food Hydrocolloids for Health

journal homepage: www.elsevier.com/locate/fhfh

Using pure Fucoidan and radiolabeled Fucoidan (99mTc-Fucoidan) as a new agent for inflammation diagnosis and therapy

Bianca Costa [a], Luana Barbosa Corrêa [a,b,c], Patrícia MachadoRodrigues e Silva [d], Yago Amigo Pinho Jannini de Sá [d], Fernanda Verdini Guimarães [d], Luciana Magalhães Rebelo Alencar [e], Rafael Loureiro Simões [a], Edward Helal-Neto [a], Eduardo Ricci-Junior [f], Maria das Graças Muller de Oliveira Henriques [b,c,*], Elaine Cruz Rosas [b,c], Ralph Santos-Oliveira [a,g]

[a] Brazilian Nuclear Energy Commission, Nuclear Engineering Institute, Laboratory of Nanoradiopharmaceuticals and Synthesis of Novel Radiopharmaceuticals, Rio de Janeiro, 21941906, Brazil
[b] National Institute for Science and Technology on Innovation on Diseases of Neglected Populations (INCT/IDPN), Oswaldo Cruz Foundation, Rio de Janeiro, 21041361, Brazil
[c] Laboratory of Applied Pharmacology, Farmanguinhos, Oswaldo Cruz Foundation, Rio de Janeiro, 21041361, Brazil
[d] Laboratory of Inflammation, Oswaldo Cruz Institute, Oswaldo Cruz Foundation, Rio de Janeiro 21040-360, Brazil
[e] Laboratory of Biophysics and Nanosystems, Federal University of Maranhão, Maranhão 65080-805, Brazil
[f] Faculty of Pharmacy, Federal University of Rio de Janeiro, Rio de Janeiro, Rio de Janeiro 21941000, Brazil
[g] Zona Oeste State University, Laboratory of Radiopharmacy and Nanoradiopharmaceuticals, Rio de Janeiro, 23070200, Brazil

ARTICLE INFO

Keywords:
Inflammation
Therapy
Radionuclide therapy
Radiopharmacy

ABSTRACT

Inflammation is a phenomenon responsible for the perturbation of homeostasis in several levels, with many sources, such as infection, injury, and exposure to contaminants. The necessity of new products that are effective in treating inflammation processes as can selectively imaging an inflammation site is a global issue. In this study, we have evaluated the applicability of Fucoidan as a therapeutic and imaging agent. We have assessed the Fucoidan in two inflammation models for therapeutic purposes: arthritis and lungs (LPS). In the case of use as an imaging agent, we evaluated the radiolabeled Fucoidan with 99mTc in inflamed lungs (LPS). The results demonstrated that Fucoidan has a therapeutic anti-inflammatory effect, especially in the lung model (LPS). Additionally, the imaging application demonstrated that radiolabeled Fucoidan (99mTc-Fucoidan) has an important chemoattraction for inflammation sites with very high bioaccumulation, which permits to think in an imaging application.

Introduction

Inflammation is a vital defense mechanism for health and is triggered by harmful stimuli such as pathogens, damaged cells, toxic compounds, or radiation, and it works by removing these stimuli to promote healing and restore homeostasis to the affected tissue (Abdulkhaleq et al., 2018; Medzhitov, 2008). The inflammatory response can lead to immunological tissue alterations, causing changes in their phenotype and cell function, with no reestablishment of normal conditions, as it leads to an adapted state of homeostasis, in which the tissue is different from the previous state, contributing to the development and aggravation of many pathologies of an inflammatory nature (Feehan & Gilroy, 2019). The early detection and assessment of inflammation sites require sensitive and non-invasive diagnostic methods. In this sense, molecular imaging modalities are fundamental tools. They allow the evaluation of tissue morphology and eventual changes due to the inflammatory process, making it possible for early treatment, improving the individual's quality of life.

Fucoidan, a general term used for a class of sulfated polysaccharides rich in α-L-fucose, negatively charged, highly hygroscopic, and soluble in water and acidic solutions found in sea cucumbers, sea urchins, and brown seaweed, has been investigated as an anti-inflammatory drug. Its structure is complex and can vary according to the species from which it is extracted, with the time and method of purification (Fletcher, Biller, Ross, & Adams, 2017; Luthuli et al., 2019). The various pharmacological effects of Fucoidan include anti-inflammatory, antiviral and antitumor activities, which are attributed to its ability to modulate some actions of the immune response through interaction with different receptors, such as Toll-like receptors (TLRs); complement receptor-3 (CR-3); and

* **All correspondence to**: Laboratory of Radiopharmacy and Nanoradiopharmaceuticals, CNEN: Comissao Nacional de Energia Nuclear, Brazil.
E-mail address: roliveira@ien.gov.br (M.d.G. Muller de Oliveira Henriques).

https://doi.org/10.1016/j.fhfh.2021.100049
Received 4 October 2021; Received in revised form 8 December 2021; Accepted 10 December 2021

scavenger receptors on dendritic cells, macrophages, and other leukocytes, as well as selecting receptors presented on platelets, leukocytes and activated endothelium (Ale, Mikkelsen, & Meyer, 2011; (Asanka-Sanjeewa et al., 2019; Carvalho et al., 2014)). It is known that Fucoidan acts at different stages of the inflammatory process, such as blockade of lymphocyte adhesion and invasion, inhibition of multiple enzymes, induction of apoptosis (Makarenkova et al., 2012). The possible mechanism of action is related to the down-regulation of MAPK and NF-κB signaling pathways followed by a decrease in pro-inflammatory cytokine production (Apostolova et al., 2020). The increasing number of investigations in the past years have demonstrated the effects of Fucoidan on the cardiovascular system (Yim & Yao, 2021), tissue regeneration (Sumayya & Kurup, 2021; Lu, HT et al., 2019), arthritis (Phull, Majid, Haq, Khan, & Kim, 2017) and pulmonary fibrosis (Wu et al., 2021), suggesting an important role of Fucoidan in the clinical treatment of several pathologies.

The use of Fucoidan as an imaging agent has been performed by Rouzet et al. (2011), who used 99mTc-labeled Fucoidan to detect the presence of platelet-rich arterial thrombi in a model of abdominal aortic aneurysms (AAAs) in rats. Recently, Vigne et al. (2019) evaluated the use of 99mTc-labeled Fucoidan as an imaging agent for early detection of myocarditis using *in vivo* model of myocarditis. In both cases, the results showed the avidity and affinity of Fucoidan for the inflammatory site and the possibility of using the radiolabeled compound as an imaging agent.

In this study Fucoidan (pure) and Fucoidan radiolabeled with 99mTc were tested to evaluate their ability as therapeutic and imaging agents in several *in vivo* models of inflammation.

Methodology

Reagents and solvents

All reagents and solvents used in all experiments were purchased from Sigma-Aldrich.

Radiolabeling with 99mTc

The labeling process was performed using 150 μg of Fucoidan, which was incubated with stannous chloride ($SnCl_2$) solution (80 μL/mL) (Sigma-Aldrich) for 20 min at room temperature, followed by the addition of 100 μCi (approximately 300 μL) of technetium-99 m.

Quality control of the labeling process with Tc-99 m

To confirm the efficacy of the radiolabeling process, Radio Thin Layer Chromatography (RTLC) was done using Whatman paper nº 1. In this regard, 2 μl of 99mTc- Fucoidan (Sigma-Aldrich) and acetone (Sigma-Aldrich) as mobile phase at times of 2 and 4 and 24 h was evaluated. The radioactivity of the strips was verified in a γ-counter (Perkin Elmer Wizard® 2470, Shelton, CT City, State). The RTLC was performed in triplicate for each time.

Animals

C57BL/6 mice, male and female (20–30 g), were obtained from Oswaldo Cruz Foundation breeding unit (Rio de Janeiro, Brazil) or the Multidisciplinary Center for Biological Research (CEMIB) (UNICAMP, São Paulo, Brazil) and housed in standard plastic cages coated with white Pinus wood shavings as bedding, and stainless-steel cover lids. Cages were maintained under controlled room temperature (23 ± 2 °C), relative air humidity (app.70%), and a 12 h light-dark cycle. All mice were kept with free access to filtered water and standard rodent chow. According to the Guide for the Care and Use of Laboratory Animals (NIH), all experiments were conducted. The Institutional Review Board and the Animal Ethics Committee approved the study protocol (CEUA UEZO 001/2015, CEUA IPEN 181/2017, CEUA FIOCRUZ LW-43/14, CEUA IOC 001/19).

Biodistribution of 99mTc-Fucoidan

Animals were injected with intravenous injection (retro-orbital sinus) of 99mTc Fucoidan (3.7 MBq/0.2 mL) and, two hours later, killed by CO_2 inhalation. Blood and several organs (heart, brain, stomach, small and large intestines, bladder, left and right lungs, left and right kidneys, liver, spleen, and pancreas) were removed and weighed. Tissue radioactive uptake was measured using a gamma counter (Wizard 2470, Perkin Elmer), and the results were expressed as a percentage of the injected dose per gram of tissue.

Uptake of 99mTc-Fucoidan in inflamed site

Animals were divided into two groups (inflamed and non-inflamed) received by installation 99mTc Fucoidan (3.7 MBq/0.2 mL) and 2 h post-injection they were euthanized by CO_2 inhalation and had both lungs (right and left) removed, weighed, and the radioactive tissue uptake measured using a gamma counter (Wizard 2470, Perkin Elmer). Results were expressed as the percentage of injected dose per gram of tissue.

Model of inflammatory arthritis

Joint Inflammation was induced by intra-articular (i.a.) injection of zymosan (500 μg/cavity) that was diluted in sterile saline to a final volume of 25 μL (Rosas et al., 2015; Correa et al., 2016). Control animals received, i.a., injection of an equal volume of sterile saline. Knee-joint swelling was evaluated by measuring the transverse diameters of each knee joint using digital calipers (Digmatic Caliper, Mitutoyo Corporation, Kanagawa, Japan). Values of knee joint thickness were expressed in millimeters (mm) as the difference of the knee-joint diameter before and after the induction of articular Inflammation (Δ). After 24 h of joint inflammation induction, the mice were euthanized using an excess of anesthetic (sodium pentobarbital 3% - Hypnol). Knee synovial cavities were washed with 300 μL of PBS containing EDTA (10 mM). Total leukocyte counts were performed in an automatic particle counter (Coulter Z2, Beckman Coulter Inc., Brea, CA, USA). Differential cell counts were performed under light microscopy (100×) using cytospin smears (Cytospin 3, Shandon Inc., Pittsburgh, PA, USA) stained according to the May–Grunwald–Giemsa method. The counts were reported as the number of cells per cavity ($\times 10^5$).

Animals were treated with Fucoidan, at a dose of 100 mg/kg, diluted in filtered water, and administered either orally (p.o.) (200 μL) or intraperitoneally (i.p.) (100 μL), 1 h before zymosan stimulation. The same volume of vehicles was administered to the control groups. Animals were divided into four experimental groups: at least five animals - i) saline-stimulated; ii) zymosan-stimulated and treated with vehicle; iii) zymosan-stimulated and treated with Fucoidan by oral route, and iv) zymosan-stimulated and treated with Fucoidan by intraperitoneal route.

Model of lung inflammation by LPS

Lung inflammation was induced in mice anesthetized with a mixture of isofluorane (0.5%) and atmospheric air by oropharyngeal aspiration of LPS (25 μg/25 μL) (from *E. coli* serotype 0127:B8; SIGMA, St. Louis, MO, USA) or sterile saline (control group). The analyses were performed 24 h after the LPS instillation. For the analysis of cells infiltrated into the airways, animals were killed with ketamine (300 mg/kg), and xylazine (30 mg/kg) and the bronchoalveolar lavage fluid (BALF) obtained after lushing the airways with twice 750 μL of PBS with ethylenediamine tetra-acetic acid (EDTA, 10 mM). BALF was retrieved and centrifuged (3000 rpm, 4 °C for 10 min), and the cell pellet was resuspended in EDTA–PBS (250 μL). Total leukocytes were counted in a Neubauer chamber using Türk solution. The differential analysis was performed in cytocentrifuged smears stained with May-Grunwald-Giemsa dye under an oil immersion objective and light microscopy (Olympus BX50). Final counts were reported as the number of cells ($\times 10^5$) per BALF.

Table 1
Percentage of labeled Fucoidan over time, after ascending chromatograms of ^{99m}Tc compared with free pertechnetate ($Na^{99m}TcO_4^-$).

Time (h)	Labeling (%)
0	99.9 ± 0.4%
1	99.9 ± 0.5%
2	99.8 ± 0.3%
4	99.8 ± 0.6%
6	99.1 ± 0.4%
24	99.6 ± 0.5%

Animals were treated with Fucoidan (100 mg/kg), diluted in filtered water, and administered intravenously, 22 h after LPS stimulation. The same volume of vehicles was distributed into the control groups. Animals were divided into three experimental groups, consisting of at least six animals: i) saline-stimulated; ii) LPS-stimulated and treated with vehicle; iii) LPS-stimulated and treated with Fucoidan.

Statistical analysis

For statistical analysis, GraphPad Prism 5.0 was used. All data are presented as mean ± SD. Two-way analysis of variance (ANOVA) followed by Bonferroni post hoc test or T-test student were used for analysis. The significance level was set at $p < 0.05$ or $p < 0.01$.

Results

Radiolabeling with 99mTc and quality control of the labeling process

The radiolabeling process using pure Fucoidan and technetium 99 metastable by a direct radiolabeling process showed to be an efficient methodology with over 95% of efficacy in 24 h (Table 1).

Biodistribution of 99mTc-Fucoidan

The biodistribution of 99mTc-Fucoidan (Fig. 1) showed a ubiquitous behavior with Fucoidan uptake in several organs. The organs that deserved more attention were: liver (Σ 29.08%), stomach (Σ 6.73%), large intestine (Σ 14.5%), kidneys (Σ 30.78%), and lungs (Σ 5.52%).

Uptake of 99mTc-Fucoidan in inflamed site

We next investigated the uptake of 99mTc-Fucoidan in inflamed tissue. As expressed in Fig. 2, it is possible to observe a higher uptake in inflamed lungs (Σ 9.79) rather than not-inflamed lungs (Σ 5,38).

Fucoidan effect on articular inflammatory response induced by zymosan

Previous reports have demonstrated that, i.a., injection of zymosan-induced, an articular inflammatory response within 24 h, characterized by a significant increase in edema formation and massive neutrophil influx (approximately 90% of total leucocytes). We examined the anti-inflammatory effects of Fucoidan in this murine model of articular inflammation and observed that mouse pretreatment with Fucoidan (100 mg/kg; i.p) 1 h before i.a. zymosan stimulation significantly impaired zymosan-induced edema formation within 24 h. However, treatment with Fucoidan did not substantially inhibit edema formation (Fig. 3A). Treatment by oral or i.p. with Fucoidan also did not deter the migration of leukocytes into the synovial cavity (Fig. 3B-D).

Fucoidan effect on lung inflammation by LPS

LPS stimulation of C57BL/6 mice yielded a significant increase in total leukocyte numbers in the BALF. The elevation in leukocyte counts was accounted for by a considerable increase in the number of neutrophils. These changes were sensitive to treatment with Fucoidan (100 mg/kg, i.v.) (Fig. 4).

Discussion

Inflammation is a vital defense mechanism for health. The early detection of the inflammation process through sensitive and non-invasive diagnostic methods allows early treatment and quality of life. Here, we observed that Fucoidan could act as a therapeutic and possible imaging agent in classical *in vivo* models of inflammation.

The direct radiolabeling process using 99mTc showed to be efficient in reducing inflammatory parameters, such as edema formation and leukocyte migration. To reach this, we conjugate Fucoidan with 99mTc that allows us to analyze the capacity of Fucoidan to act as a therapeutic and imaging agent. In this context, the presence of several reactive groups, including alkyl groups and sulfo groups in the structure of Fucoidan, aids in the conjugation reaction with 99mTc, especially in [99mTc = O^{3+}] or [99mTc$(CO_3)]^+$ core configuration. The [99mTc = O^{3+}] is the most common core used for radiolabeling with 99mTc complexes. In this reaction, due to the presence of sulfo groups, the 99mTc would assume a square pyramidal geometry, with the technetium (99mTc) in the middle of the structure. In the case of [99mTc$(CO_3)]^+$ with the reaction occurring with the methyl group of the structure, probably an octahedral geometry with 99mTc in the middle of the structure will be formed to stabilize the charges and density of the complex (Costa, Ilem-Özdemir, & Santos-Oliveira, 2019). In both cases, a stable and effective complex of Fucoidan and 99mTc will be formed.

The biodistribution assay indicates the usefulness and effectiveness of the radiopharmaceutical. This assay allows for evaluating and quantifying the radiopharmaceutical uptake in tissues and determining how it is excreted from the body (Duatti, 2021). In this study, we showed higher uptake of Tc-99m-labeled Fucoidan in kidneys (30.78%) and liver (29.08%), while in other viscera organs, the uptake was lower. The uptake in the large intestine was 14.5%, 6.73% in the stomach, and 5.52% in the lungs. As the liver and kidney uptake was very similar, it is impossible to confirm whether the radiopharmaceutical excretion was predominant in the hepatobiliary or the kidneys system. Even so, the kidney system eliminated a significant fraction, which is an interesting route due to lower radiation exposure. However, complementary studies should be done to determine the time of renal clearance. In confirming so, this radiopharmaceutical could be useful for obtaining dynamic images for morphological imaging (Chigoho, Bridoux, & Hernot, 2021). In addition, the higher uptake in this organ can be advantageous for other clinical applications. Tan J et al. (2020) describes the use of Fucoidan to treat nephrotic syndrome, including a Fucoidan-based drug approved by the Chinese Food and Drug Administration in 2003 for the treatment of kidney disease (Wang, Geng, Yue, & Zhang, 2019.

As mentioned above, we show in this study that there was also a significant uptake of 99mTc-labeled Fucoidan in the liver. The elimination of this radiopharmaceutical through the hepatobiliary system could measure liver function and potentially identify patients at risk for liver failure. This could provide valuable information in the pre-and postoperative estimation of patients with hepatobiliary disease (Hoekstra et al., 2013; Lambie et al., 2011). Also, due to the affinity of 99mTc-labeled Fucoidan for the lower gastrointestinal tract, this radiopharmaceutical could be used to provide images for diagnosis and follow-up of inflammatory bowel disease characterized by recurrent local Inflammation (Dmochowska & Wardill, 2018). We propose that 99mTc- conjugated Fucoidan could be used as a non-invasive technique to treat several in-

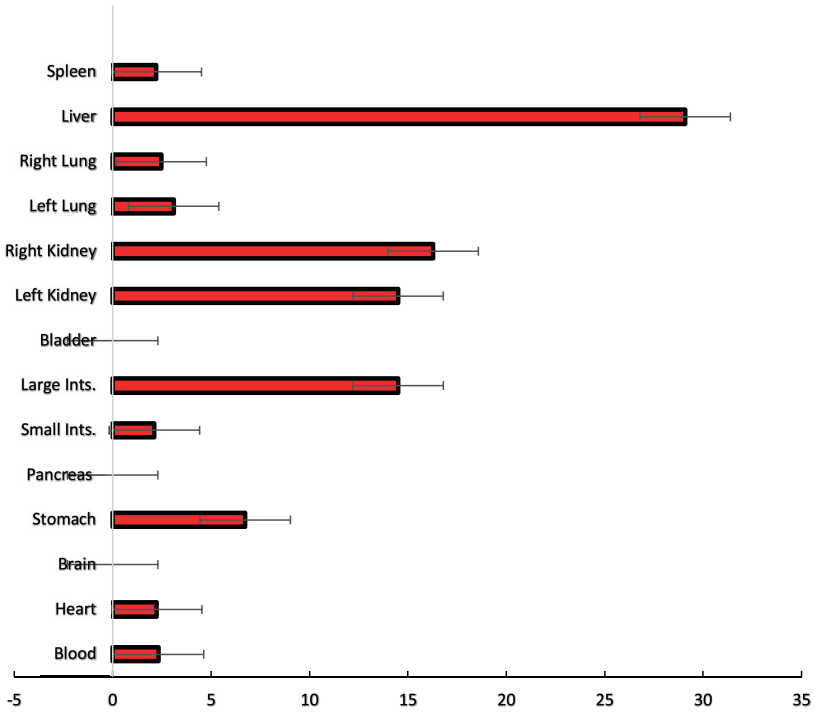

Fig. 1. Biodistribution of 99mTc-Fucoidan in healthy animals. Animals were injected with intravenous injection of 99mTc Fucoidan (3.7 MBq/0.2 mL). Blood and several organs were removed and weighed. Tissue radioactive uptake was measured using a gamma counter, and the results were expressed as a percentage of the injected dose per gram of tissue.

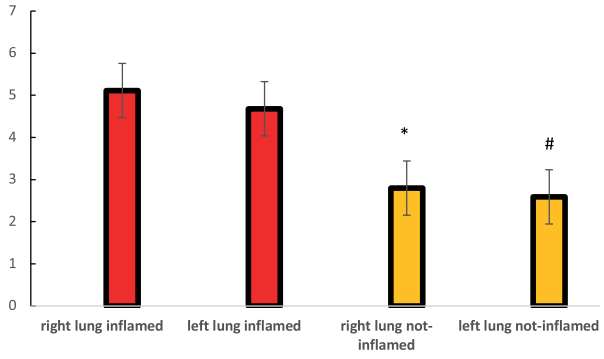

Fig. 2. Lung uptake of 99mTc Fucoidan showing the higher uptake in inflamed lungs. Lung inflammation was induced by oropharyngeal aspiration of LPS (25 μg /25 μL), and 99mTc Fucoidan (3.7 MBq/0.2 mL) was instilled. 2 h post-installation, both lungs (right and left) were removed, weighed and the radioactive tissue uptake was measured using a gamma counter. Results were expressed as the percentage of injected dose per gram of tissue. * $p < 0,01$ when compared to right lung inflamed; # $p < 0,01$ when compared to left lung inflamed.

flammatory pathologies, which would be more comfortable for the patient during the treatment period.

Non-invasive imaging techniques such as magnetic resonance imaging (MRI), single-photon emission computed tomography (SPECT), and positron emission tomography (PET) is widely used for assessing disease activity and monitoring response to treatment. The Radionuclide-based SPECT and PET images have advantages over other modalities because they provide molecular function information, high sensitivity, and high contrast (Lee, Ehlerding, & Cai, 2019; MacRitchie et al. 2020). The development of SPECT and PET imaging for chronic inflammatory diseases has three main targets that can be classified into different categories: (1) cell adhesion molecules; (2) surface markers on immune cells; and (3) cytokines or enzymes (Lee et al., 2019).

Saboural et al. (2014) labeled Fucoidan with 99mTc for developing a molecular imaging agent to diagnose acute coronary syndrome in rats with transient myocardial ischemia. In an experimental model of autoimmune myocarditis, 99mTc-labeled Fucoidan was used to access the inflammation site early. SPECT/CT with 99mTc-labelled Fucoidan accurately diagnosed the inflammatory process in the early stages of autoimmune myocarditis. This study showed the great potential of 99mTc-labeled Fucoidan in monitoring the evolution of this disease and the effectiveness of therapy (Vigne et al., 2020).

These works corroborate the results obtained in this study regarding the use of this sulfated polysaccharide as an imaging agent. We demonstrated a great uptake of Tc-99m-labeled Fucoidan in inflamed lungs (Σ 9.79) compared to the uptake in healthy lungs (Σ5.38). This difference could be related to the affinity of Fucoidan to bind specific targets in the inflammatory site. The results obtained clearly show a lower migration of leukocytes to the area of inflammation, both articular and pulmonary.

Another mechanism that may explain the anti-inflammatory action is the ability of Fucoidan to modulate the immune response through the inhibition of pro-inflammatory signaling pathways, such as mitogen-activated protein kinases (MAPK) and nuclear factor-κB (NF-κB) (Tsay et al., 2021; Wang et al., 2019; Pradhan et al. 2019; Manikandan et al., 2020). It was shown that Fucoidan inhibits LPS-induced inflammation via blocking NF-κB and MAPK pathways

Fucoidan is presumed to bind to specific glycoprotein receptors on the surface of macrophages, dendritic cells, and other leukocytes such as TLR4 receptors; CD14; CR3; SR1. This can result in the downregulation of genes related to this pathway, inhibiting the expression of pro-inflammatory cytokines and other processes regulated by them, such as NF-kB (Lin et al., 2018; Lin et al., 2020). For example, Fucoidan can inhibit tumor cell migration and lymphocytes recruitment by suppressing CCL22 in M2 macrophages via NF-κB-dependent transcription. Data from this study showed that oral administration of Fucoidan did not significantly inhibit zymosan-induced edema formation.

Many authors have evaluated the anti-inflammatory activity of Fucoidan in different experimental models, applying it via gavage or adding it to the animals' feed, as shown in Table 2 below.

In these studies, Fucoidan was administered orally for a certain period, which may have contributed to the positive results described in them. On the other hand, the anti-inflammatory action reported in this

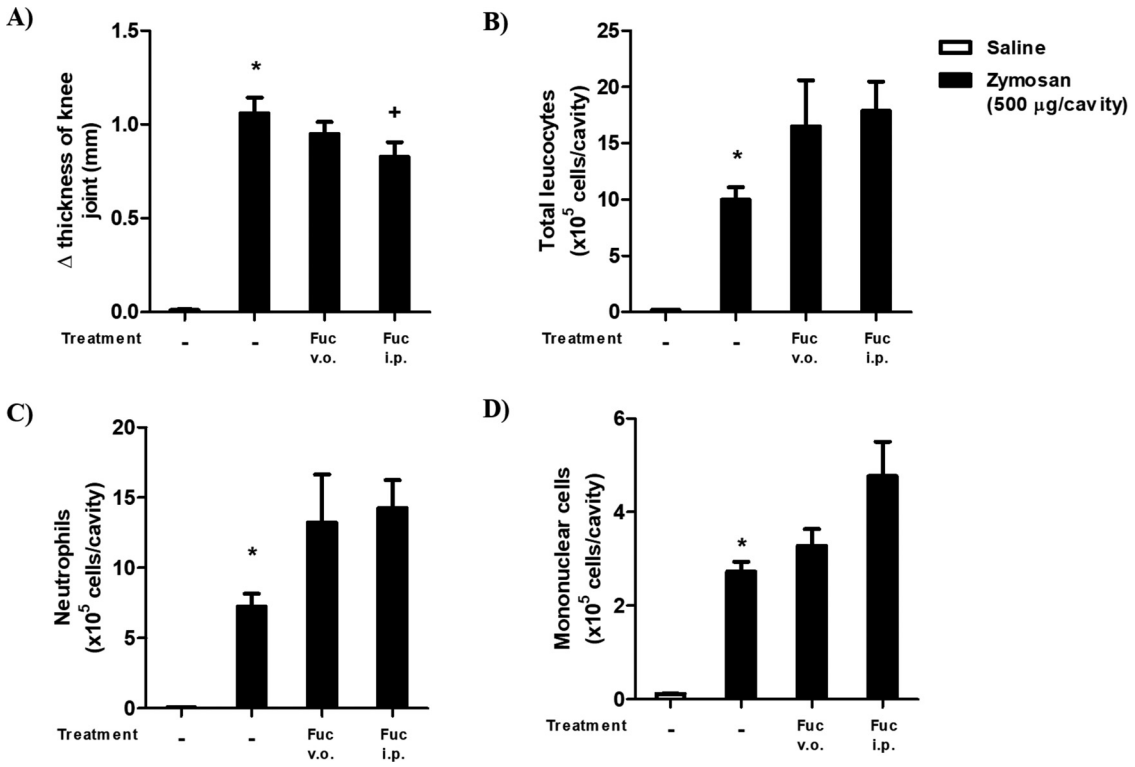

Fig. 3. Fucoidan effect on edema and leukocyte migration during zymosan-induced arthritis. (A) Knee joint thickness was measured with a digital caliper before and 24 h after zymosan stimulation. Mice were pretreated with fucoidan (Fuc) (100 mg/kg) orally or intraperitoneally 1 h before stimulation, and after 24 h of zymosan, i.a. injection (500 μg/25 μL/cavity), knee synovial cells were recovered and analyzed in (B) total leukocyte, (C) neutrophils and (D) mononuclear cells migration. Control animals received sterile saline, i.a., injection (25 μL/cavity). Data were presented as mean ± SEM ($n = 6$). Statistically significant ($P \leq 0.05$) are indicated between stimulated and non-stimulated groups (*) and between treated and non-treated groups (+).

Table 2
Anti-inflammatory activity of orally administered Fucoidan.

Disease	Treatment with fucoidan	Outcomes	Mechanisms	Reference
Radiation Pneumonitis	200 mg/kg/day oral gavage for 14 days	Attenuated induced fibrosis; decreased leukocyte accumulation	Changed the expression Patterns of inflammatory cytokines	Yu et al., 2018
Formalin induced paw-edema	50 mg/kg/day oral gavage for 7 days	Anti-nociceptive effect and decreased the size of paw swelling edema	Retained p65/nf-κb transcription factor showing downregulation of expression of pro-inflammatory mediators	Manikandan et al., 2020
Thioacetaide-induced Liver injury	20 mg/kg/day by oral gavage for 42 days	Hepatoprotective effect suppression of the inflammatory responses and acting as an antioxidant	Hepatic antioxidative enzymes; and a lower alt, ast, tnf-α, il-1β, and c-reactive protein	Tsai et al., 2021
Surgically induced endometriosis	50–150 mg/kg/day by oral gavage for 42 days.	anti-inflammatory effects; reduced the volume and weight of endometriotic lesions	Inhibited the viability and migration; decreased inflammatory cytokines and VEGF	Chang et al., 2020

study, in which the anti-inflammatory action of orally administered Fucoidan was not expressive, can be justified by the low frequency of administration of this polysaccharide right before the induction of edema with zymosan, or it could be that the model used not ideal, as the zymosan model produces an acute inflammatory response and substances that mainly interfere with innate immunity tend to be more successful.

Finally, based on the evidence available, the Fucoidan mechanism is widely known (Table 3). They can mimic the P-selectin glycoprotein ligand-1 (PSGL-1), exhibiting a high affinity for P-selectin over expressed by activated platelets consequently blocking P-selectin (Bachelet et al., 2009). P-selectin is a cell surface adhesion molecule which mediates leukocyte-endothelial cell adhesion (Cheng et al., 2020). P-selectin is stored in membranes of a granules of platelets and Weibel-Palade bodies of endothelial cells. When mediators such as thrombin or histamine activate these cells, the granules fuse with the plasma membrane and P-selectin is rapidly redistributed to the cell surface. P-selectin interacts reversibly with PSGL-1, a trans-membrane homodimeric mucin on leukocytes. These interactions mediate leukocyte rolling on activated platelets and endothelial cells. So, P-selectin initiates leukocyte recruitment during inflammation (Panicker et al., 2017). Due to the activation of the inflammatory process in the lung by LPS or in the joint by zymosan, there is probably an overexpression of P-selectin, which justifies accumulation of 99mTc-Fucoidan in the inflammatory site. Thus, a functional radiolabeled compound as with ligands for tar-

Table 3
Studies on the mechanism of action of Fucoidan.

System	Indication	Fucoidan functions	Method	Results	Reference
Nano drug delivery system (NDDS) (MnO2/uPA@pep-Fuco)	Thrombolytic therapy	Surface modification to improve poor water dispersibility and low biocompatibility of MnO2 NPs	Thrombin-responsive peptide (GGLVPRGFGG, pep) as the bridge to connect MnO2 NPs and Fucoidan	NDDS specifically accumulate at platelet-rich thrombus because of the ligand-receptor interaction between Fuco and P-selectin.	Zhang et al., 2021
Nanoparticle-based drug delivery systems	Thrombosis	Fu can strongly bind to activated platelet-rich thrombi through P-selectin-based ligand–receptor interactions	To ensure targeted delivery of Uk and ICG to a thrombus site, we used Fu as an activated platelet-specific ligand to modify the Uk/ICG@Si-AuNR nanocomposite	P-selectin specific Si-AuNR nanocomposite can efficiently and safely deliver ICG and Uk to thrombi with photothermal/e zymatic thrombolytic effects and NIR II fluorescence imaging function (ICG) for thrombosis imaging and therapy	Chang et al., 2021
P-selectin-specific complex nanoparticles (CNPs)	in vitro MR imaging of inflammatory endothelial cells model	Lower molecular weight fucoidan (LMWF) inhibited P-selectin binding, and modulated P-selectin and provided with other biological functions including promotion of revascularization and endothelial protective activities	Combine LMWF (LMWF8775, thermolysin-hydrolyzed protamine peptide (cell penetrating peptide, TPP1880) and Gd-DTPA in a nanosystem for in vitro MR imaging of inflammatory endothelial cells model	The nanoplatform integrating multiple functionalities such as P-selectin targeting, cell penetrating, and MR imaging in the CNPs can selectively deliver Gd-DTPA to PMA-stimulated, activated HUVECs	Cheng et al., 2020
Fucoidan-functionalized dextran submicroparticles (SPs)	in vitro amidolytic and fibrinolytic activities	Fucoidan emerged as an affordable, high-quality targeting ligand to P-selectin that was prior validated by the group on various polysaccharide-based nano- & microsystems for molecular diagnostics and targeted therapy	Fabricated novel fucoidan-functionalized dextran submicroparticles (SPs) by a green chemistry method using fully biodegradable and biocompatible compounds, all of them approved by the FDA.	Fucoidan functionalized SPs have a high and specific affinity to P-selectin and accumulate on activated platelet aggregates and bind to the thrombi in vivo and proved superior in vivo thrombolytic efficacy in a mouse stroke thrombin model	Zenych et al. 2021
Biospecific polysaccharide-based submicronic particles (SPs)	Evaluate the cytotoxicity, contrast properties and targeting capacity of the obtained objects	Able to bind to human activated platelets for atherothrombosis imaging by MRI	SPs were synthesized by co-crosslinking of fucoidan and former dextran macrocomplexes within 110 the droplets of a water-in-oil emulsion	Particles exhibited good colloidal stability and were cytocompatible with human endothelial cells and exhibited good MR contrast properties	Forero Ramirez et al., 2020

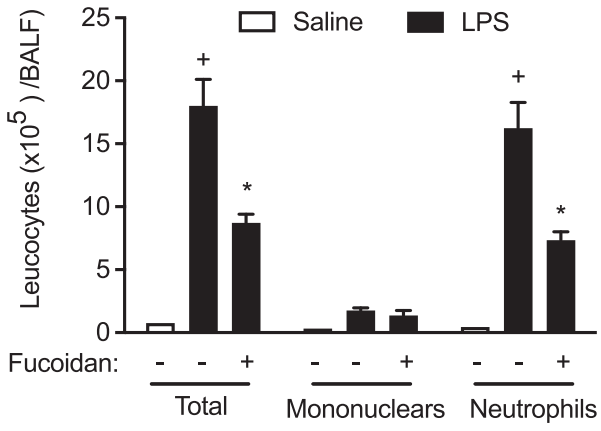

Fig. 4. Effect of treatment with Fucoidan (100 mg/kg) on LPS-induced leucocyte changes (total and differential cell counts) in the BALF. The bronchoalveolar lavage fluid from C57BL/6 mice was collected 24 h after LPS (25 μg) stimulation. Values are mean ± SEM from at least six animals. $^{+}P < 0.05$ as compared with saline-stimulated mice. $^{*}P < 0.05$ as compared with LPS-stimulated mice.

geting P-selectin can be used to deliver imaging and therapeutic agents for treatments of the diseases associated with increased expression of P-selectin.

Conclusion

In this study, we demonstrated for the first time that Fucoidan could act as an imaging agent in inflammatory models. There is already a phase 1 clinical trial reporting the first human evaluation of 99mTc-labeled Fucoidan SPECT for P-selectin imaging, demonstrating a good biodistribution and safety profile (Zheng et al., 2019). To date, two clinical trials are ongoing. These trials are focused on the biodistribution and tolerance of Fucoidan. Healthy volunteers are involved in trials involving the biodistribution, safety, and dosimetry of a labeled Fucoidan (ClinicalTrials.gov, Identifier: NCT03422055). In another trial, patients with stage III-IV non-small cell lung cancer (NSCLC) are being studied (in a placebo-controlled trial), in which Fucoidan is added to their chemotherapy treatment to determine the impact it would have. Present in your quality of life (ClinicalTrials.gov, Identifier: NCT03130829). The results of these studies (clinical trials) will play an important role in obtaining information about ADME and Fucoidan toxicity in humans. Although Fucoidan extracts have not been approved for biomedical pur-

poses, research on the bioactivity of this compound has increased exponentially in recent years, with a focus on its application as drug delivery agents, biomaterials, and therapeutic agents.

Declaration of Competing Interest

No potential conflicts of interest relevant to this article exist.

Acknowledgement

Dr. Ralph Santos-Oliveira would like to thank the financial support from Carlos Chagas Filho Foundation for Research Support of Rio de Janeiro State (FAPERJ) (E-26/201.946/2020, E-26/200.815/2021 and 26/010.000981/2019) and CNPq (301069/2018-2).

References

Abdulkhaleq, L. A., Assi, M. A., Abdullah, R., Zamri-SaadY, M., Taufiq-Yap, H., & Hezmee, M. N. M. (2018). The crucial roles of inflammatory mediators in inflammation: A review. *Veterinary World, 11*, 627–635. 10.14202/vetworld.2018.627-635.

Ale, M. T., Mikkelsen, J. D., & Meyer, . S. (2011). Important determinants for fucoidan bioactivity: A critical review of structure-function relations and extraction methods for fucose-containing sulfated polysaccharides from brown seaweeds. *Marine Drugs, 9*, 2106–2130. 10.3390/md9102106.

Apostolova, E., Lukova, P., Baldzhieva, A., Katsarov, P., Nikolova, M., Iliev, I., et al. (2020). Immunomodulatory and anti-inflammatory effects of fucoidan: A review. *Polymers, 12*, 2338. 10.3390/polym12102338.

Asanka-Sanjeewa, K. K., Jayawardena, K. T., Kim, H. S., Kim, S. Y., Shanura, I. P., Wang, L., et al. (2019). Fucoidan isolated from Padina commersonii inhibit LPS-induced Inflammation in macrophages blocking TLR/NF-κB signal pathway. *Carbohydrate Polymers, 15*, 224 *Article 115195*. 10.1016/j.carbpol.2019.115195.

Carvalho, A. C. S., Sousa, R. B., Franco, A. X., Costa, J. V. C., Neves, L. M., Ribeiro, R. A., et al. (2014). Protective effects of Fucoidan, a P- and L-selectin inhibitor, in murine acute pancreatitis. *Pancreas, 43*, 82–87. 10.1097/MPA.0b013e3182a63b9d.

Chang, L. C., Chiang, Y. F., Chen, H. Y., Huang, Y. J., Liu, A. C., & Hsia, S. M. (2020). The potential effect of Fucoidan on inhibiting epithelial-to-mesenchymal transition, proliferation, and increase in apoptosis for endometriosis treatment: In vivo and in vitro study. *Biomedicines, 8*, 1–15. 10.3390/biomedicines8110528.

Chang, L. H., Chuang, E. Y., Cheng, T. M., Lin, C., Shih, C. M., Wu, A. T., et al. (2021). Thrombus-specific theranostic nanocomposite for codelivery of thrombolytic drug, algae-derived anticoagulant and NIR fluorescent contrast agent. *Acta Biomaterialia, 134*, 686–701 Oct 15. 10.1016/j.actbio.2021.07.072.

Cheng, T. M., Li, R., Kao, Y. J., Hsu, C. H., Chu, H. L., Lu, K. Y., et al. (2020). Synthesis and characterization of Gd-DTPA/fucoidan/peptide complex nanoparticle and in vitro magnetic resonance imaging of inflamed endothelial cells. *Materials Science & Engineering. C, Materials for Biological Applications, 114*, Article 111064 Sep;. 10.1016/j.msec.2020.111064.

Chigoho, D. M., Bridoux, J., & Hernot, S. (2021). Reducing the renal retention of low- to moderate-molecular-weight radiopharmaceuticals. *Current Opinion in Chemical Biology, 63*, 219–228. 10.1016/J.CBPA.2021.06.008.

Correa, L. B., Pádua, T. A., Seito, L. N., Costa, T. E., Silva, M. A., Candéa, A. L., et al. (2016). Anti-inflammatory effect of methyl gallate on experimental arthritis: Inhibition of neutrophil recruitment, production of inflammatory mediators, and activation of macrophages. *Journal of Natural Products, 79*, 1554–1566. 10.1021/acs.jnatprod.5b01115.

Costa, B., Ilem-Özdemir, D., & Santos-Oliveira, R. (2019). Technetium-99 m metastable radiochemistry for pharmaceutical applications: Old chemistry for new products. *Journal of Coordination Chemical, 72*, 1759–1784. 10.1080/00958972.2019.1632838.

Dmochowska, N., & Wardill, H.R. (.2018). Advances in imaging specific mediators of inflammatory bowel disease. 1–13 doi:10.3390/ijms19082471

Feehan, K. T., & Gilroy, D. W. (2019). Is resolution the end of inflammation? *Trends in Molecular Medicine, 25*, 198–214 Epub 2019 Feb 19. 10.1016/j.molmed.2019.01.006.

Fletcher, H. R., Biller, ., Ross, A. B., & Adams, J. M. M. (2017). The seasonal variation of Fucoidan within three species of brown macroalgae. *Algal Research, 22*, 79–86.

Forero Ramirez, L. M., Gobin, E., Aid-Launais, R., Journe, C., Moraes, F. C., Picton, L., et al. (2020). Gd(DOTA)-grafted submicronic polysaccharide-based particles functionalized with fucoidan as potential MR contrast agent able to target human activated platelets. *Carbohydrate Polymers, 245*, Article 116457. 10.1016/j.carbpol.2020.116457.

Hoekstra, L.T., .Graaf, W., de, Nibourg, G.A.A., Heger, M., Bennink, R.J., .Stieger, B. et al. (2013). Physiological and biochemical basis of clinical liver function tests. *Ann Surg.* 257, 27–36. doi:10.1097/SLA.0b013e31825d5d47.

Lambie, H., Cook, A. M., Scarsbrook, A. F., Lodge, J. P. A., Robinson, P. J., & Chowdhury, F. U. (2011). Tc 99 m - hepatobiliary iminodiacetic acid (HIDA) scintigraphy in clinical practice. *Clinical Radiology, 66*, 1094–1105. 10.1016/j.crad.2011.07.045.

Lee, H. J., Ehlerding, E. B., & Cai, W. (2019). Antibody-based tracers for PET/SPECT imaging of chronic inflammatory diseases. *Chembiochem : A European Journal of Chemical Biology, 20*, 422–436. 10.1002/cbic.201800429.

Lin, Y., Qi, X., Liu, H., Xue, K., Xu, S., & Tian, Z. (2020). The anti-cancer effects of Fucoidan: A review of both in vivo and in vitro investigations. *Cancer Cell International, 20*, 1–14. 10.1186/s12935-020-01233-8.

Luthuli, S., Wu, S., Cheng, Y., Zheng, X., Wu, M., & Tong, H. (2019). Therapeutic effects of Fucoidan: A review on recent studies. *Mar Drugs., 17*(9), 487. 10.3390/md17090487.

Makarenkova, I. D., Logunov, D. Y., Tukhvatulin, A. I., Semenova, I. B., Zvyagintseva, T. N., Gorbach, V. I., et al. (2012). Sulfated polysaccharides of brown seaweeds are ligands of toll-like receptors. *Biochemistry Moscow Suppliment Series., 6*, 75–80. 10.1134/S1990750812010118.

Manikandan, R., Parimalanandhini, D., Mahalakshmi, K., Beulaja, M., Arumugam, M., Janarthanan, S., et al. (2020). Studies on isolation, characterization of Fucoidan from brown algae Turbinaria decurrens and evaluation of it's in vivo and in vitro anti-inflammatory activities. *International Journal of Biological Macromolecules, 160*, 1263–1276. 10.1016/j.ijbiomac.2020.05.152.

Medzhitov, R. (2008). Origin and physiological roles of inflammation. *Nature, 454*, 428–435. 10.1038/nature07201.

Panicker, S. R., Mehta-D'souza, P., Zhang, N., Klopocki, A. G., Shao, B., & McEver, R. P. (2017). Circulating soluble P-selectin must dimerize to promote inflammation and coagulation in mice. *Blood, 130*(2), 181–191 Jul 13. 10.1182/blood-2017-02-770479.

Phull, A. R., Majid, M., Haq, I., Khan, M. R., & Kim, S. J. (2017). In vitro and in vivo evaluation of anti-arthritic, antioxidant efficacy of Fucoidan from Undaria pinnatifida (Harvey) Suringar. *International Journal of Biological Macromolecules, 97*, 468–480. 10.1016/j.ijbiomac.2017.01.051.

Saboural, P., Chaubet, F., Rouzet, F., Al-Shoukr, F., Azzouna, R. B., Bouchemal, N., et al. (2014). Purification of a low molecular weight fucoidan for SPECT molecular imaging of myocardial infarction. *Marines Drugs, 12*, 4851–4867. 10.3390/MD12094851.

Sumayya, A. S., & Kurup, G. M. (2021). In vitro anti-inflammatory potential of marine macromolecules cross-linked bio-composite scaffold on LPS stimulated RAW 264.7 macrophage cells for cartilage tissue engineering applications. *Journal of Biomaterials Science, Polymer Edition, 32*, 1040–1056. 10.1080/09205063.2021.1899590.

Tsai, M. Y., Yang, W. C., Lin, C. F., Wang, C. M., Liu, H. Y., Lin, C. S., et al. (2021). The ameliorative effects of Fucoidan in thioacetaide-induced liver injury in mice. *Molecules (Basel, Switzerland), 26*. 10.3390/molecules26071937.

Vigne, J., Cognet, T., Guedj, K., Morvan, M., Merceron, O., Louedec, L., et al. (2020). Early detection of localized immunity in experimental autoimmune myocarditis using [99mTc]Fucoidan SPECT. *Molecular Imaging Biology, 22*, 643–652. 10.1007/s11307-019-01420-8.

Wang, J., Geng, L., Yue, Y., & Zhang, Q. (2019). *Use of fucoidan to treat renal diseases : A review of 15 years of clinic studies*: Vol. 163 (1 ed.). Amsterdam, Netherlands: Elsevier Inc..

Wu, N., Li, Z., Wang, J., Geng, J., Yue, Y., Deng, Z., et al. (2021). Low molecular weight fucoidan attenuating pulmonary fibrosis by relieving inflammatory reaction and progression of epithelial-mesenchymal transition. *Carbohydrate Polymers, 273*, Article 118567. 10.1016/j.carbpol.2021.118567.

Y, Yao, & Yim, E. K. F. (2021). Fucoidan for cardiovascular application and the factors mediating its activities. *Carbohydrate Polymers, 270*, Article 118347. 10.1016/j.carbpol.2021.118347.

Yu, H. H., Chengchuan, E. K. O., Chang, C. L., Yuan, K. S. P., Wu, A. T. H., Shan, Y. S., et al. (2018). Fucoidan inhibits radiation-induced pneumonitis and lung fibrosis by reducing inflammatory cytokine expression in lung tissues. Marine Drugs **2018**, *16*, 1–14. 10.3390/md16100392.

Zhang, H., Qu, H., He, Q., Gao, L., Zhang, H., Wang, Y., et al. (2021). Thrombus-targeted nanoparticles for thrombin-triggered thrombolysis and local inflammatory microenvironment regulation. *Journal of Controlled Release : Official Journal of the Controlled Release Society, 339*, 195–207 Nov 10. 10.1016/j.jconrel.2021.06.043.

Zheng, K. H., Kaiser, Y., Poel, E., Verberne, H., Aerts, J., Rouzet, F., et al. (2019). 99Mtc-Fucoidan as diagnostic agent For P-selectin imaging: first-in-human evaluation (Phase I). *Atherosclerosis, 287 Article e143*. 10.1016/j.atherosclerosis.2019.06.425.